Conditional Attribution of the 2018 Summer Extreme Heat over Northeast China: Roles of Urbanization, Global Warming and Warming-induced Circulation Changes

Chunlüe Zhou[1], Deliang Chen[2], Kaicun Wang[3], Aiguo Dai[1], and Dan Qi[4]

[1]Department of Atmospheric and Environmental Sciences, University at Albany, State University of New York, 1400 Washington Avenue, Albany, New York 12222, USA

[2]Regional Climate Group, Department of Earth Sciences, University of Gothenburg, Gothenburg, 40530, Sweden

[3]College of Global Change and Earth System Science, Beijing Normal University, Beijing, 100875, China

[4]National Meteorological Center, China Meteorological Administration, Beijing, 100081, China

Corresponding Author: Dr. Chunlüe Zhou, E-mail: chunluezhou@gmail.com

Submitted to *Bulletin of the American Meteorological Society*

(Ref.: BAMS-D-19-0197)

Capsule

The probability of the record-breaking summer heat of 2018 over Northeast China was increased by a combination of human-caused climate change influences on thermodynamics and circulation, and urbanization.

Introduction

The averaged near-surface air temperature (T_a) of July-August 2018 over Northeast China is ~1.73°C above the 1971-2000 mean, the highest since 1961; and one third of the stations in the region broke the historical record (Figs. 1a and 1b), which posed a great threat to local ecosystems and human health because this region has seldom experienced such extreme heats in previous decades (Chen et al. 2019).

In addition to influences from global warming, summer hot days over Northeast China are typically accompanied by local anticyclonic anomalies (Chen et al. 2019; Wu et al. 2011), which provides favorable conditions for increased solar radiation-induced diabatic heating due to reduced cloud cover and subsidence-induced adiabatic heating (Chen and Lu 2015; He et al. 2018). Therefore, relative contributions from atmospheric circulation anomaly and global warming to the probability of such extreme summer heats are first investigated.

More importantly, we further quantify contributions of warming-induced circulation changes to such summer heats. Global warming may induce atmospheric circulation changes, which in turn can influence the intensity and frequency of heat waves (Horton et al. 2015; Zhou et al. 2019). However, few studies have quantified this effect, likely due to weak signal of climate change compared with large natural variability in atmospheric circulation. Thanks to acceptable performance of CMIP5-simulated circulations at monthly timescales (Figs. S1 and S2), we make such an attempt to estimate the contribution from warming-induced circulation changes to the 2018 summer heat. Besides, urban heat island effect makes T_a over urban areas

higher than that of rural regions (Zhou et al. 2019), which could intensify summer heats. The contribution from urbanization to the 2018 summer heat is also examined in this study.

Therefore, this study tries to answer three questions: 1) How does the extreme summer heat of 2018 over Northeast China look like in a historical context? 2) How much does an anticyclone contribute to the 2018 summer heat? And 3) what are relative roles of urbanization, global warming and warming-induced circulation changes in forming the 2018 summer heat?

Data and methods

Daily T_a from 1961 to 2018 at ~690 meteorological stations over Northeast China (Fig. 1a) were collected (http://data.cma.cn/). The T_a dataset has undergone quality control tests including outlier and duplicates identification, and spatial and temporal consistency checks (Zhou et al. 2018).

Based on Ren et al. (2015) and Zhou et al. (2019), thirty rural stations (stars in Fig. 1a) were identified in comparison with urban stations for quantifying the effect of urbanization (Sun et al. 2016). The latest stable night lights in 2013 from the defense meteorological satellite program (http://ngdc.noaa.gov/eog/dmsp) were further used to show urban (light index >15) and rural regions (≤15). July-August 2018 circulation anomaly regime (Fig. 1c) was depicted by the 2.5°×2.5° 500-hPa geopotential height (Z500) from NCEP-R1 (https://www.esrl.noaa.gov/) (Kalnay et al. 1996).

CMIP5 model outputs (Taylor et al. 2011) (http://cmip-pcmdi.llnl.gov/cmip5/)

were used to quantify human influences on the probability of the 2018 summer heat. We first tested probability distributions of July-August T_a and Z500 anomalies from the CMIP5 historical all-forcings (ALL) simulations against observations via a Kolmogorov-Smirnov test (p>0.05). Second, we assessed and selected the ALL simulations with a significant positive temporal correlation (p<0.05) between the detrended July-August T_a and Z500 anomalies. As a result, 40 out of 54 simulations from eleven models were selected for this study, with the ALL runs extended through 2018 using the RCP4.5 runs (58×40 samples) (Sun et al. 2016) and the corresponding natural-forcings-only runs (NAT) ending in 2012 (52×40 samples; Table S1). Detailed timeseries can be seen in Fig. S1.

To separate contributions from global warming and warming-induced circulation changes to the probability of the 2018 summer heat, following Christidis and Stott (2015), we defined years with CMIP5-based circulation regimes in individual model runs similar to the observed in July-August 2018 (i.e., a deep anticyclone within black rectangle in Fig. 1c) as high correlation years (pattern correlation $\geqslant$ 0.5; CMIP5 multi-model mean Z500 anomalies in Fig. 1d; more details in Fig. S2), and defined neutral years with pattern correlations of -0.1 to 0.1. We realized that global warming in ALL runs will increase Z500 over most of globe including Northeast China, and such a background change in Z500 may not necessarily intensity the anomalous anticyclonic circulation over Northeast China, which requires further investigation. Therefore, Z500 anomalies gradient was adopted to provide a better measure of the change in the circulation strength in this study.

To be consistent, observation and model data were converted into anomalies relative to 1971-2000 mean; and first re-gridded onto thirty 2.5°×2.5° grids and then area-averaged over the study region (110°E-130°E, 35°N-50°N, Fig. 1a). Several statistical techniques were exploited:

1) Following Schaller et al. (2016), Generalized Pareto Distribution (GPD) with a properly selected threshold was used to fit the July-August T_a and Z500 anomalies.

2) Probability Ratio [$PR1=P_{(Ta\text{-}urban|urban)}/P_{(Ta\text{-}urban|rural)}$] was first calculated to quantify urbanization effect in the likelihood of the 2018 summer heat (defined as $\geqslant$ 1.73°C averaged in urban regions over Northeast China). Here, $P_{(Ta\text{-}urban|urban)}$ and $P_{(Ta\text{-}urban|rural)}$ represent the probabilities of T_a anomalies exceeding 1.73°C in urban and rural scenarios.

3) After excluding the urban heat island effect, another $PR2=P_{(Ta\text{-}rural|ALL\text{-}highZ500)}/P_{(Ta\text{-}rural|ALL\text{-}neutralZ500)}$ was calculated to estimate the role of an anticyclone existence in the probability of the 2018 summer heat. Here, $P_{(Ta\text{-}rural|ALL\text{-}highZ500)}$ and $P_{(Ta\text{-}rural|ALL\text{-}neutralZ500)}$ represent the probabilities of T_a anomalies to exceed 1.64°C (averaged in rural regions) under the high and neutral Z500 regimes in the ALL runs. $PR3=P_{(Ta\text{-}rural|ALL\text{-}highZ500)}/P_{(Ta\text{-}rural|NAT\text{-}highZ500)}$] was used to quantify the influence of global warming (i.e., human-induced thermodynamical contribution). To further quantitively estimate the role of anthropogenic warming-induced circulation changes (i.e., human-induced dynamical contribution), we applied Bayesian statistics (Gelman et al. 2013; Yiou 2017) to modify PR as $PR4=[P_{(ALL\text{-}highZ500)}/P_{(NAT\text{-}highZ500)}]\cdot[P_{(highZ500|NAT\text{-}Ta\text{-}rural)}/P_{(highZ500|ALL\text{-}Ta\text{-}rural)}]$. Here,

$P_{(Ta\text{-}rural|NAT\text{-}highZ500)}$ represents the probability of T_a anomaly to exceed 1.64°C under the high Z500 regime in NAT runs; and $P_{(highZ500|ALL\text{-}Ta\text{-}rural)}$ and $P_{(highZ500|NAT\text{-}Ta\text{-}rural)}$ represent the probabilities of circulation anomaly regimes similar to the 2018 observed regime when such extreme summer heats (≥1.64°C) occur in ALL and NAT runs. 95% confidence intervals (CI) were estimated with a 1000-member bootstrap (with replacement) (Efron and Tibshirani 1986).

Results

Role of the Anticyclone

In 2018 summer, the 5880-metres contour of the western Pacific subtropical high moved northwestward and brought the record-breaking anticyclone anomaly over Northeast China (black square in Fig. 1b) (Chen et al. 2019), leading to the record-breaking summer heat of 2018 over both urban and rural areas (Figs. 1a-b). New daily T_a records were registered at stations near the center of the anomalous anticyclone (black dots in Fig. 1a). Fig. 1c shows strong correlations between the detrended July-August T_a and Z500 anomalies (associated with local anticyclones) with correlation coefficient (r) of 0.71 (p=0.00) in the study region (Fig. 1e).

The likelihoods of the 2018 summer heat in high-correlation years (with the pattern shown in Fig. 1d) and neutral years in ALL runs are 11% (20 out of 224 samples) and 2% (8 out of 437 samples), respectively (Fig. 2a). In other words, an anomalous anticyclone could increase the PR to 6 (95% CI: 4 - 9, Fig. 2d).

Influence of the Urbanization

The record-breaking July-August T_a anomalies of 2018 not only occurred in the urban areas (averaged 1.73°C, black-edged circles in Fig. 1a), but also at rural stations (averaged 1.64°C, black-edged pentagrams in Fig. 1a). A Student's *t*-test of temperature differences in 2018 between the 2.5°×2.5° urban and rural grids shows a significance level of 0.07. The metropolitan area has vast built-up surfaces and frequent human activities, leading to higher temperatures than at rural stations (Fig. 1b). A GPD fit of the observed July-August T_a anomalies suggests that the 2018 extreme summer heat is a 1-in-60-year event (95% CI: 30-500) for the urban regions and a 1-in-80-year event (95% CI: 40-10^5) for the rural regions (Fig. 1f).

Compared with the probabilities of T_a anomaly exceeding 1.73°C in urban and rural scenarios (based on PR1; Fig. 1f), urbanization increases the PR to 1.17 (95% CI: 1-10^2) (Fig. 2e), i.e., ~17% increase in the likelihood.

Influences of Global Warming and Warming-induced Circulation Changes

July-August T_a anomalies over Northeast China significantly correlate with July-August global-mean temperature (r=0.56, p=0.00) (Fig. 1e), implying a strong footprint of global warming on the 2018 summer heat over Northeast China.

Compared with the probabilities of T_a anomaly exceeding 1.64°C under similar circulation regimes in ALL and NAT runs (based on PR3; Fig. 2a), we found that global warming has increases the probability by ~78% (95% CI: 53-128%; Fig. 2f).

Global warming has been argued to have caused atmospheric circulation changes that have altered regional extreme events in different ways (Horton et al. 2015; Schär et al. 2004; Zhou and Wang 2016), increasing attribution challenge of human-induced

dynamical and thermodynamical contributions to odds of the event.

The probabilities of CMIP5-simulated circulation regimes similar to the 2018 observed regime over Northeast China, i.e., with pattern correlations being 0.5 or more, are almost equivalent in ALL and NAT runs (Fig. 2b), but the intensity of the circulation anomalies in high-correlation years increases by ~11% in ALL runs relative to NAT runs (mean of 2.29 vs. 2.07 metres/^{o}lat described by Z500 anomaly gradient in Fig. 2c). These results imply that global warming has altered the Z500 field by strengthening the anomalous anticyclone over Northeast China, which in turn may has enhanced the severity of the 2018 summer heat.

Compared with the probabilities of T_a anomaly exceeding 1.64°C and circulation regimes similar to the 2018 observed regime in ALL and NAT runs (based on PR4), we found that an increased likelihood by ~27% (95% CI: 12%-59%) is attributable to the warming-induced circulation intensity change over Northeast China, while the warming-induced circulation frequency change has no significant impact on the likelihood (Fig. 2f).

Conclusions and Discussion

Our analyses of surface observations and reanalysis fields indicate the record-breaking temperature and circulation anomalies in 2018 summer over Northeast China. Return period of the 2018 summer heat is 1-in-60-years for the urban areas and 1-in-80-years for the rural areas. CMIP5-based analyses suggest that the existence of an anomalous anticyclone over Northeast China increases the odds of

the 2018 summer heat to 6.16 times that without such an anticyclone.

Based on the GPD fits, we found that urbanization over the metropolitan areas might has increased the likelihood of the 2018 summer heat by ~17%. After excluding the urbanization effect, CMIP5-based PR analyses suggest that anthropogenic global warming may has increased the probability of the 2018 summer heat over Northeast China by ~78%. Global warming has strengthening the anticyclonic circulation by ~11%, which may has increased the likelihood (by ~27%) of the 2018 summer heat over Northeast China.

In summary, an anomalous anticyclonic circulation over Northeast China was the main cause of the 2018 summer heat. Global warming and warming-induced circulation intensity change have increased the odds, and urbanization has further exacerbated the 2018 summer heat over Northeast China.

The non-stationarity of the time series would consistently increase the attribution uncertainties for all the factors (Fig. 2d-e), but it does not change our main conclusions.

Acknowledgments This study was supported by National Key R&D Program of China (2017YFA0603601), the National Natural Science Foundation of China (41525018), the U.S. National Oceanic and Atmospheric Administration (NA18OAR4310425), and the Swedish VR (2017-03780), STINT (CH2015-6226), and MERGE. A. Dai was also supported by the National Science Foundation (AGS-1353740 and OISE-1743738), the U.S. Department of Energy's Office of

Science (DE-SC0012602), and the U.S. National Oceanic and Atmospheric Administration (NA18OAR4310425). We thank Dr. Nikos Christidis, Dr. Stephanie Herring and Dr. Andrew King for their insightful suggestions.

References:

Chen, R., and R. Lu, 2015: Comparisons of the Circulation Anomalies Associated with Extreme Heat in Different Regions of Eastern China. *J. Clim.*, **28,** 5830-5844.

Chen, R., Z. Wen, and R. Lu, 2019: Influences of tropical circulation and sea surface temperature anomalies on extreme heat over Northeast Asia in the midsummer of 2018. *Atmos. Oceanic Sci. Lett.*, **12,** 238-245.

Christidis, N., and P. A. Stott, 2015: Extreme rainfall in the United Kingdom during winter 2013/14: the role of atmospheric circulation and climate change. *Bull. Am. Meteorol. Soc.*, **96,** 46-50.

Efron, B., and R. Tibshirani, 1986: Bootstrap methods for standard errors, confidence intervals, and other measures of statistical accuracy. *Stat Sci*, **1,** 54-75.

Gelman, A., H. S. Stern, J. B. Carlin, D. B. Dunson, A. Vehtari, and D. B. Rubin, 2013: *Bayesian data analysis.* Chapman and Hall/CRC.

He, Y., K. Wang, C. Zhou, and M. Wild, 2018: A revisit of global dimming and brightening based on sunshine duration. *Geophys. Res. Lett.*, **45,** L077424.

Horton, D. E., N. C. Johnson, D. Singh, D. L. Swain, B. Rajaratnam, and N. S. Diffenbaugh, 2015: Contribution of changes in atmospheric circulation patterns to extreme temperature trends. *Nature*, **522,** 465-469.

Kalnay, E., and Coauthors, 1996: The NCEP/NCAR 40-year reanalysis project. *Bull. Am. Meteorol. Soc.*, **77,** 437-471.

Ren, G., and Coauthors, 2015: An integrated procedure to determine a reference station network for evaluating and adjusting urban bias in surface air temperature data. *J. Appl. Meteorol. Climatol.*, **54,** 1248-1266.

Schär, C., P. L. Vidale, D. Lüthi, C. Frei, C. Häberli, M. A. Liniger, and C. Appenzeller, 2004: The role of increasing temperature variability in European summer heatwaves. *Nature*, **427,** 332-336.

Schaller, N., and Coauthors, 2016: Human influence on climate in the 2014 southern England winter floods and their impacts. *Nature Clim. Change*, **6,** 627-634.

Sun, Y., X. Zhang, G. Ren, F. W. Zwiers, and T. Hu, 2016: Contribution of urbanization to warming in China. *Nature Clim. Change*, **6,** 706-710.

Taylor, K. E., R. J. Stouffer, and G. A. Meehl, 2011: An overview of CMIP5 and the experiment design. *Bull. Am. Meteorol. Soc.*, **93,** 485-498.

Wu, R., S. Yang, S. Liu, L. Sun, Y. Lian, and Z. Gao, 2011: Northeast China summer temperature and North Atlantic SST. *J. Geophys. Res. D Atmos.*, **116,** D16116.

Yiou, P., 2017: A statistical framework for conditional extreme event attribution. *Adv. Stat. Clim. Meteorol. Oceanogr.*, **3,** 17-31.

Zhou, C., and K. Wang, 2016: Coldest temperature extreme monotonically increased and hottest extreme oscillated over northern hemisphere land during last 114 years. *Sci. Rep.*, **6,** 25721.

Zhou, C., Y. He, and K. Wang, 2018: On the suitability of current atmospheric reanalyses for regional warming studies over China. *Atmos. Chem. Phys.*, **18,** 8113-8136.

Zhou, C., K. Wang, D. Qi, and J. Tan, 2019: Attribution of a record-breaking heatwave event in summer 2017 over Yangtze River Delta. *Bull. Am. Meteorol. Soc.*, **100,** 97-103.

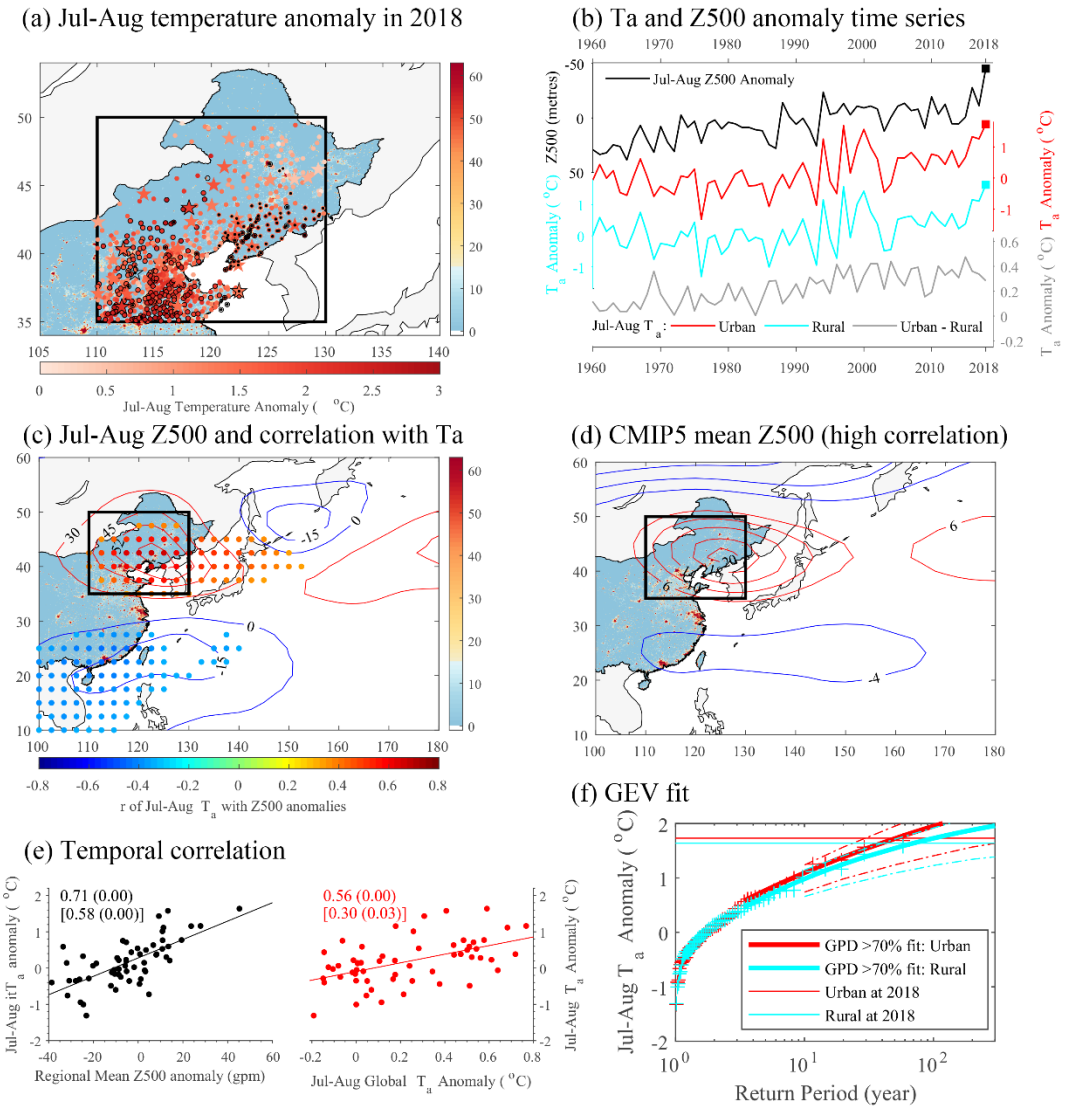

Fig. 1 (**a**) Spatial pattern of the observed July-August temperature (T_a) anomalies in 2018 over Northeast China. Stations having record-breaking July-August (daily) temperatures in 2018 summer since 1961 are marked with black edges (dots). Urban and rural stations are plotted as color-filled circles and pentagrams. **(b)** Timeseries of Z500 anomalies (in black) over the study region, and T_a over urban (in red), rural regions (in cyan) and their difference (in light black), relative to the period 1971-2000. Squares represents broken records in 2018. **(c)** Circulation regime in July-August 2018 (in red/blue contours). Correlations between the detrended region-averaged T_a

and gridded Z500 are shown as color-filled circles (p<0.01). **(d)** CMIP5-multi-ensemble-mean Z500 anomalies under high-correlation regimes from 40 ALL simulations. **(e)** Scatterplots of T_a with Z500 and global-mean T_a. Correlations were calculated before and after detrending (coefficients and significance levels in square brackets). **(f)** GDP fit (in solid) of T_a.

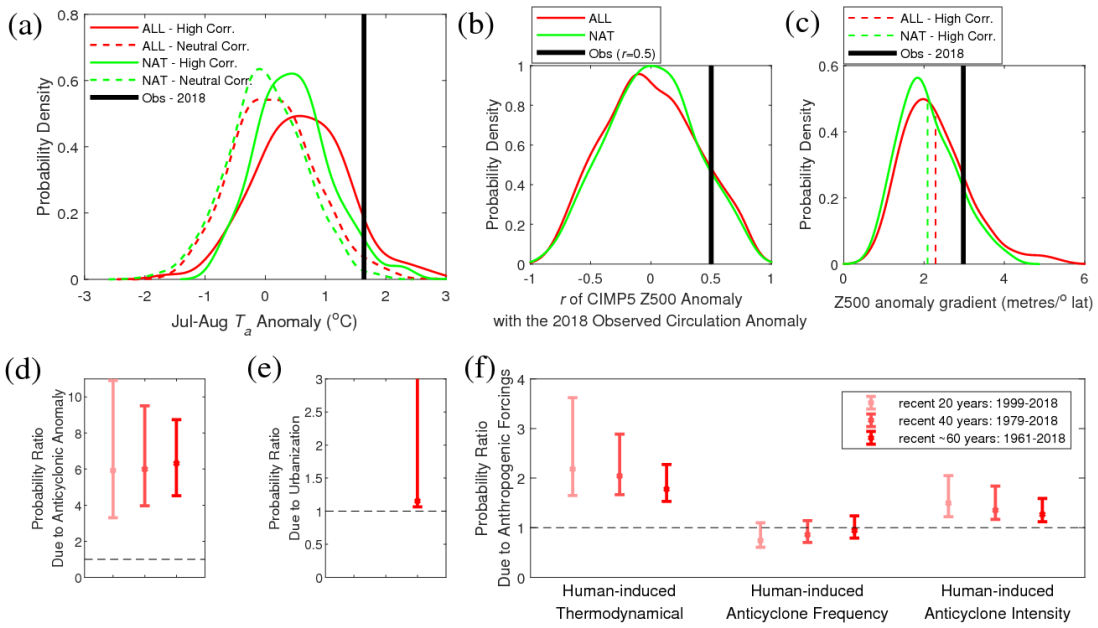

Fig. 2 (**a**) Probability density of July-August temperature anomalies (T_a) under high (in solid) and neutral (in dash) regimes in 40 all-forcings (ALL, in red) and natural-forcing-only (NAT, in green) simulations. Black thick line is the observed T_a of July-August 2018 over rural region. **(b)** Probability density of pattern correlation coefficients (r) between CMIP5-based Z500 regimes and the 2018 observed regime in ALL/NAT runs. **(c)** Probability density of Z500 anomaly gradients with r>0.5. Dash lines are their mean. **(d)** Probability ratio (PR) of the 2018 summer heat due to the occurrence of anticyclone. **(e)** PR due to urbanization. **(f)** PR due to human influences from human-induced dynamical (frequency and intensity) and thermodynamical changes.